Simulation of aerosol fields over South Asia using CHIMERE – part-I: spatio-temporal characteristics and heterogeneity

N. Srivastava[1,*], S. K. Satheesh[2,3], Nadege Blond[4] and K. Krishna Moorthy[5]

[1]Department of Physics, Birla Institute of Technology, Mesra, Ranchi 835 215, India
[2]Centre for Atmospheric and Oceanic Sciences, Indian Institute of Science, Bengaluru 560 012, India
[3]Divecha Centre for Climate Change, Indian Institute of Science, Bengaluru 560 012, India
[4]Laboratoire Image Ville Environnement, UMR7362 CNRS, Université de Strasbourg, Strasbourg, France
[5]ISRO HQ, Antariksh Bhavan, Bengaluru 560 231, India

In order to understand the regional climate implications of aerosols over Indo-Gangetic Plains (IGP), a major Indo-US field experiment, Ganges Valley Aerosol Experiment (GVAX) was conducted during 2011–12. Atmospheric Radiation Measurement (ARM) mobile facility (AMF) was deployed at the northern Indo-Gangetic Plain over the high-altitude site, Manora Peak, Nainital (29°21′33.84″N, 79°27′29.27″E, 1980 m amsl) in Central Himalayas, for an year-round measurement of aerosols, clouds and other climate-relevant atmospheric parameters. One of the objectives of GVAX was examining the ability of models to simulate aerosols over Indian region and validate the simulations. In part-1 of this two-part paper, we examine use of the chemical transport model 'CHIMERE' to simulate aerosol fields over Indian region (4–37.5°N; 67–88.5°E) for multiple years (2006, 2007 and 2008) by simulating the spatial and temporal distribution of PM10, BC mass concentrations and OC/BC ratios. It is seen that the model successfully captures the broad features of the regional distribution of aerosols, including the most conspicuous IGP hotspot and its seasonality.

Keywords: Aerosols, black carbon, chemistry transport model, CHIMERE, GVAX.

Introduction

FOR realistic climate impact assessment of aerosols, information on their spatial and temporal variations is essential[1,2]. Several sources of data exist for this purpose such as ground-based observations, satellite data and chemistry-transport model simulations[3–5]. For global and even regional scale analyses, ground-based observations are inadequate (as they are not dense enough and evenly distributed) and satellite data provides only a snapshot and that too with during cloud-free period and still have limitations especially over the landmass. As such, chemistry transport models are handy for constructing regional, seasonal and global aerosol distributions. Earlier models incorporated only the transport and dispersion of aerosols, but of late, consistent revisions and addition of new processes have led to development of more complex models, which include photochemical reactions and the formation of secondary aerosols[6,7]. The availability of high speed computing systems has enhanced the speed of modelling studies and improved the performance of the models[8]. Currently, chemistry transport models can perform simulations with a spatial resolution ranging from 1 to 200 km. Despite their limited spatial coverage, ground-based measurements provide accurate data against which the model simulations could be compared and validated at different time scales. Once validated, the models are specially suited for application over large spatial domains, where it is not feasible to maintain dense observational sites.

In the backdrop of the above, we have examined the ability of CHIMERE chemical transport model in simulating aerosol characteristics over India. In this exercise, we have simulated the spatio-temporal distribution of the mass concentration of total particulate matter (PM_{10}), black carbon (BC), aerosol optical depth (AOD) and the ratio (OC/BC) of organic carbon to black carbon over Indian sub-continent. The purpose of choosing this model for the above exercise has been its better ability to simulate shorter scale variations[9], the wide use of this model as an air pollution forecast model and being used in Europe as a part of the national air pollution forecasting system[10–15]. Besides, the model runs over a range of spatial scales from the regional scale to (several thousand km) to the urban scale (100–200 km) with a resolution of 100 km to 1–2 km. Its ability to reproduce the concentration of ozone at various European regions has been repeatedly demonstrated[10–12].

Model specifications and simulation domain

The 3D-chemistry transport model CHIMERE version Chimere 2008c (refs 5, 10) is used in this study. This

*For correspondence. (e-mail: nishi.bhu@gmail.com)

model is designed to produce daily forecast of aerosols and trace pollutants. A detailed description of the model and boundary condition is available in the literature[5,16–18] and as such, only a brief description is given below.

CHIMERE is a portable model with interfaces (such as MM5, WRF and ECMWF) to use different types of meteorological data, boundary conditions and emission inventories as inputs. Boundary conditions are available from MOZARD and/or LMDz-INCA models and aerosol boundary conditions are specified based on GOCART global simulations[19,20]. The Global Land Cover Facility (GLCF) database has been utilized for land use[21] and the biogenic emissions are based on the land cover. In the present study, the MM5 model has been used to generate meteorological input files and AVN/NCEP FNL data have been used to force the MM5 model. The spatial grid resolution of the MM5 was ½ × ½ degree.

We used a single domain simulation over India and the region of interest ranged from (3.25–38.75°N; 64.75–97.25°E) with a central grid at (21°N, 81°E) and with 8 vertical levels extending from surface to 500 hPa (Figure 1). The horizontal transport of chemical species is treated using three different schemes, namely Parabolic Piecewise Method (PPM, a three order horizontal scheme)[22], the Godunov scheme[23] and the simple upwind first-order scheme. Van Leer scheme is preferred due to its good accuracy and low computational cost. Vertical transport is integrated in the model using first order UPWIND scheme. In model calculations horizontal mixing is not taken into account while vertical turbulent mixing is considered in the boundary layer[24]. To represent aerosols depending on their size distribution and compositions the sectional approach given by Gelbard and Seinfeld[25] has been used. Six aerosol sizes are represented as 'bins' in the model. Dry deposition, wet deposition and secondary aerosol formation are considered[26–28]. For anthropogenic emission, we have developed an interface with EDGAR 3.2 fast Track 2000 dataset. This dataset incorporates anthropogenic emission of Kyoto Protocol greenhouse gases (CO_2, CH_4, N_2O and F-gases HFCs, PFCs and SF10) and air pollutants (CO, NMVOC, NO_x, SO_2) for the year 2000 on global scale.

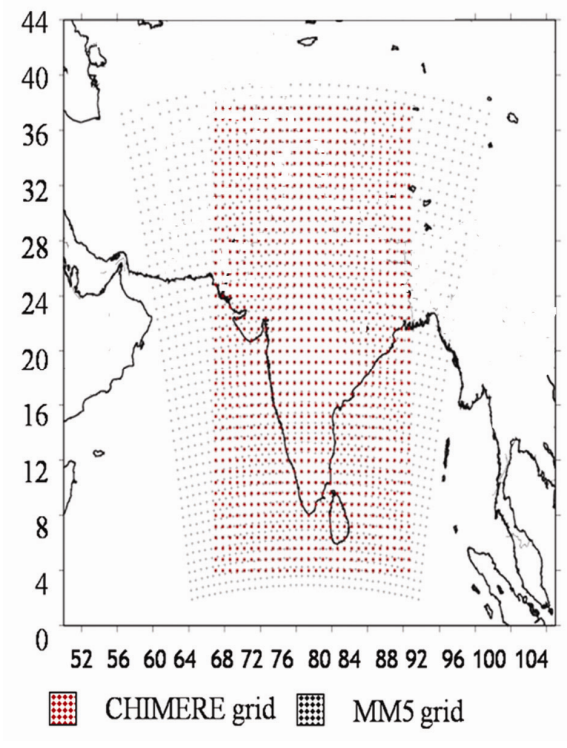

Figure 1. Grid points of MM5 and CHIMERE model grid domain.

Results

CHIMERE simulations

Spatio-temporal variations of simulated PM_{10}. Figure 2 shows the simulated spatial distribution of monthly mean columnar PM_{10} (from surface to 500 hPa) for 2006–2008 over Indian landmass and adjoining oceans. During dry, winter months (October–February) modelled PM_{10} concentration, integrated over all heights, was highest over the Indo-Gangetic basin with values as high as ~600 μg m^{-2}. These values were consistent with those reported earlier[29–34] using satellite-derived and ground-measured data. During pre-monsoon (Mar–May) and summer monsoon months (June–September), aerosol concentration over the western coast was much higher compared to the rest of India. Over oceanic region, the concentration of particulate matter was much higher over the Arabian Sea (AS), compared to the Bay of Bengal (BoB), depicting the transport of dust from west Asia adding to the *in situ* produced sea-salt, as has also been acknowledged[35–37]. In winter months over AS, aerosol mass concentration ranges from ~200 to 300 μg m^{-2} and over BoB it reached only up to ~100 μg m^{-2}. The concentration was higher closer to the coast and decreased rapidly as we move to farther oceanic regions due to reduction in the continental influence. As winter retreat, the concentration of particulate matter decreased over the Indo-Gangetic basin and over the oceanic regions as well. With the start of pre-monsoon season, a thick plume of dust developed over the western part of India and the average concentration of PM_{10} increased all over the land portion of the domain whereas over the oceanic region the concentration decreased compared to the previous months. The concentrations were now comparable over the eastern and western coasts and increased further in subsequent months and reaching, within the plume, as high as ~900 μg m^{-2}. With the onset of summer monsoon in June, the PM_{10} concentration falls rapidly over the southern tip with

simulated values less than ~100 μg m^{-2}. This effect spreads across the entire mainland with the advance of monsoon, except over the western arid and desert regions of Rajasthan, where the rainfall is meagre (http://www.imd.gov.in/section/nhac/dynamic/Normalrf_jul.gif) and dust storms persist. Consequently, the spatial extent of high PM_{10} has shrunk and the peak concentration remained high. Over large portion of the domain, PM_{10} concentration remained as low as ~50 μg m^{-2} during July. Moving on to August and September (Figure 2 *h–i*), the spatial area of dust plume continues to shrink and finally disappears due to the combined effects of wet removal and reduced source impacts (local and advected from the west).

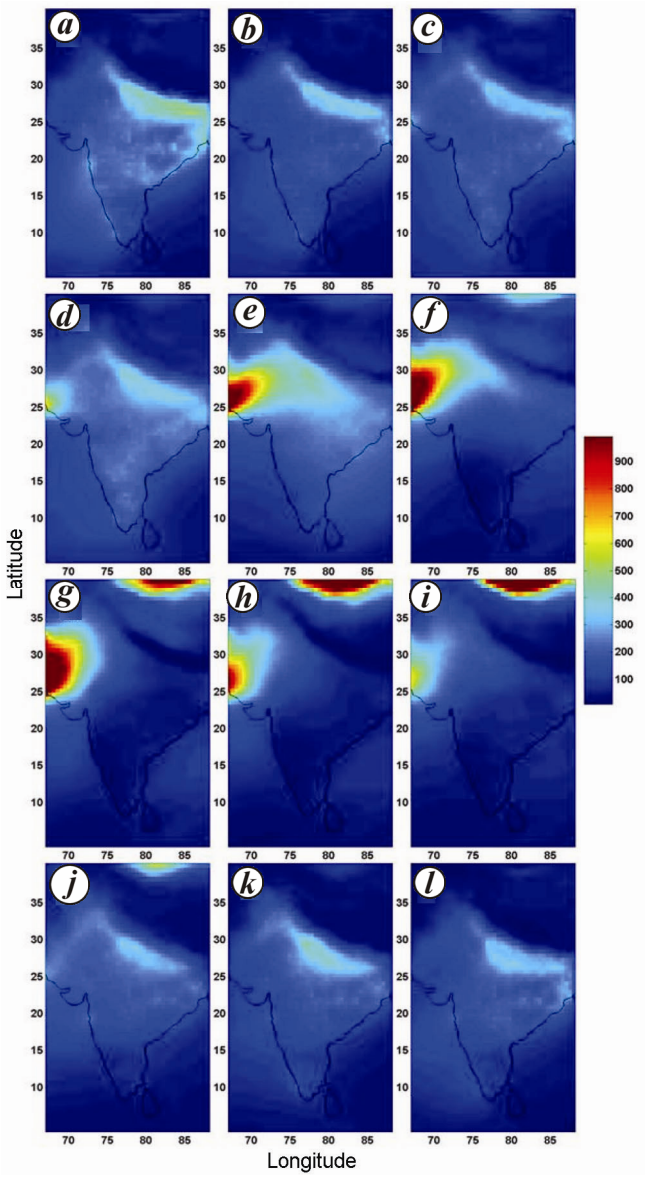

Figure 2. Spatial distribution of model-simulated monthly mean (2006–2008) PM10 concentration (units: μg m^{-2}) over Indian continent and adjacent oceanic regions; ***a–l*** represent months of January to December respectively.

Spatio-temporal heterogeneity in simulated black carbon

Black carbon (BC), generated by the incomplete/low temperature combustion of fossil fuel and biomass, is the strong light absorbing component of the carbonaceous aerosols and thus has strong relevance to climate forcing, besides its health impacts[38–42]. The spatio-temporal distribution of monthly mean simulated columnar averaged BC (averaged for 2006–2008) over the model domain (Figure 3) reveals:

- Temporally, BC concentration remains in excess of ~20 μg m^{-2} over most of the Indian landmass during the dry months from October to April, the highest being in

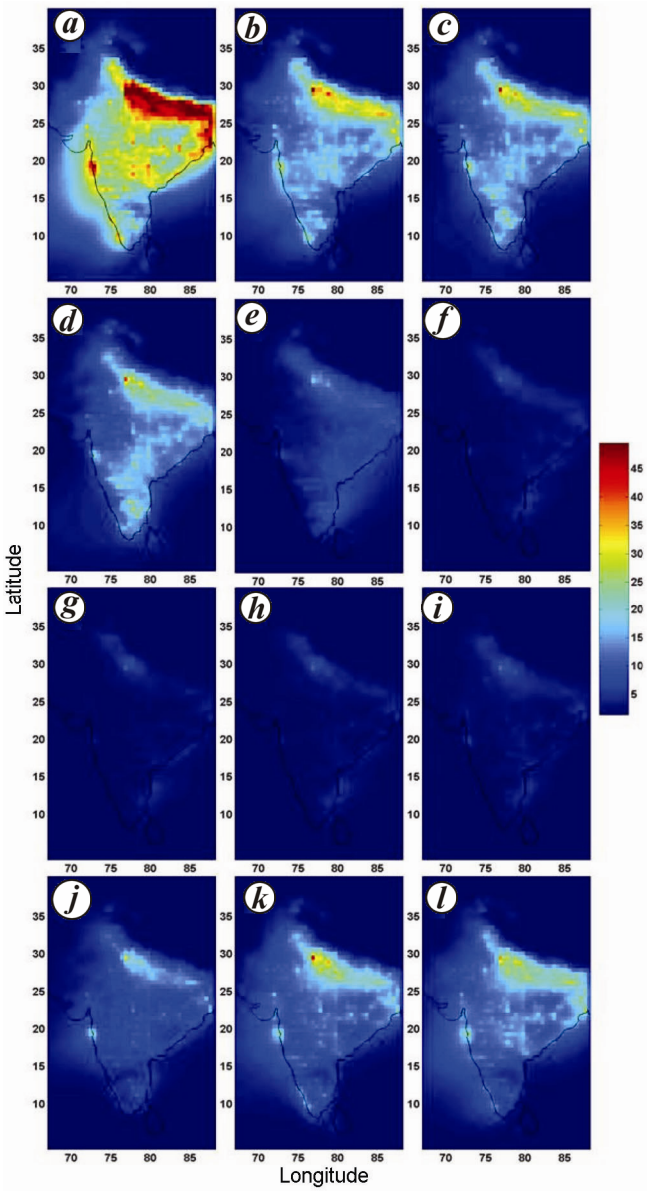

Figure 3. Same as figure 2; but for black carbon mass concentration (unit: μg m^{-2}).

January (Figure 3 *a*) when values were more than 45 μg m^{-2} over the IGP and at several pockets in the Central and Western regions of Indian landmass. The entire coastal belt also depicts high values of BC, but lower than those in the IGP. Moderately high concentrations are seen even over significant parts of AS and BoB.

- From May, the concentration decreases rapidly, and during the wet months of June to September (Figure 3 *f–i*) the concentration is remarkably low over the entire domain (values ≤ ~5 μg m^{-3}).
- Spatially, the IGP (lat. >25°N and long. >76°E) exhibits the highest values in all the months. Hotspots of high BC values are seen around mega-cities (such as Mumbai, Delhi, Hyderabad and Kolkatta) also.

Such a spatial distribution, with high BC mass concentrations over the Indo-Gangetic basin, has been reported in the past[33,43–50], even though the magnitudes differed. During a mobile campaign of 2004, using instrumented vehicles, Moorthy *et al.*[1] have shown high concentrations of BC over coastal regions of India, with higher concentration over the east coast than on the west coast. Over the northern Indian region, the remarkably low temperature, coupled with frequent occurrence of fog, the shallow atmospheric boundary layer resulting from the weak thermal convection, and the western disturbances are shown to contribute to the high BC concentrations near the surface during the winter time[33]. The advection of cold meteorological fronts from the west is shown leading to suppression of vertical dispersion and enhancement of BC during winter. The peculiar orography of these plains with mountains and plateaus on the north and south also favours piling up of local and advected pollutants.

The lower concentration seen over the oceans arises due to absence of local sources. During summer, the concentration of BC, though decreased over the whole region (Figure 3 *e*), the Indo-Gangetic basin and eastern coastal India still depicted high values. This seasonal change arises from increased solar heating and the consequent rise in land temperature resulting in deeper atmospheric boundary layer (ABL) during these months (in comparison to winter), which favours rapid dilution of the surface concentration due to better vertical dispersion and ventilation. Over the AS region, BC concentration remains much lower than that over the BoB. During the monsoon months (June to September, Figure 3 *f–i*) the effect of the widespread rainfall leads to rapid decrease in BC over the whole domain. After the withdrawal of monsoon, the belt of high BC concentration starts developing again over the IGP. In summary, CHIMERE was able to simulate qualitatively the broad features of BC distributions expected and reported for this region.

Simulated OC/BC ratio. Carbonaceous aerosols contain BC and organic carbon (OC), having contrasting radiative effects, and as such, their relative abundance assumes importance[51]. Climate models often tend to use unrealistic values of OC/BC over the Indian region[52]. An OC/BC ratio in the range 1–2 indicates dominance of fossil fuel-based emissions, while larger values occur in emissions from biomass burning[52–55]. Throughout the year, over the IGP, simulated OC/BC ratio was around 1.0, suggesting the primary sources for carbonaceous aerosol to be fossil fuel combustion; probably vehicular emissions and coal fired thermal plants and industries[51,52]; while over the rest of India the ratio was around 2.0. The near-non-seasonality of this ratio indicated a general prevalence of fossil fuel generated BC over the domain, similar to that reported by Novakov *et al.*[56] over other locations such as Japan, Europe, China and North America. Examining the finer details for the month of January (when the aerosol load in general was highest over the domain) in Figure 4, it emerges that over the western coast the ratio increases gradually towards ocean from its value of ~2.0 at the coast. Similarly, over the east coast the low OC/BC at the coast increases drastically (from 2 to 3.5) as we move to farther oceanic regions. To get an idea about the frequency of occurrence of OC/BC ratio we have selected a threshold as 2.0. We have estimated the number of occurrences when OC/BC ≤ 2.0 and when OC/BC < 2.0 (Figure 5). These plots give the monthly average number counts for years 2006–08.

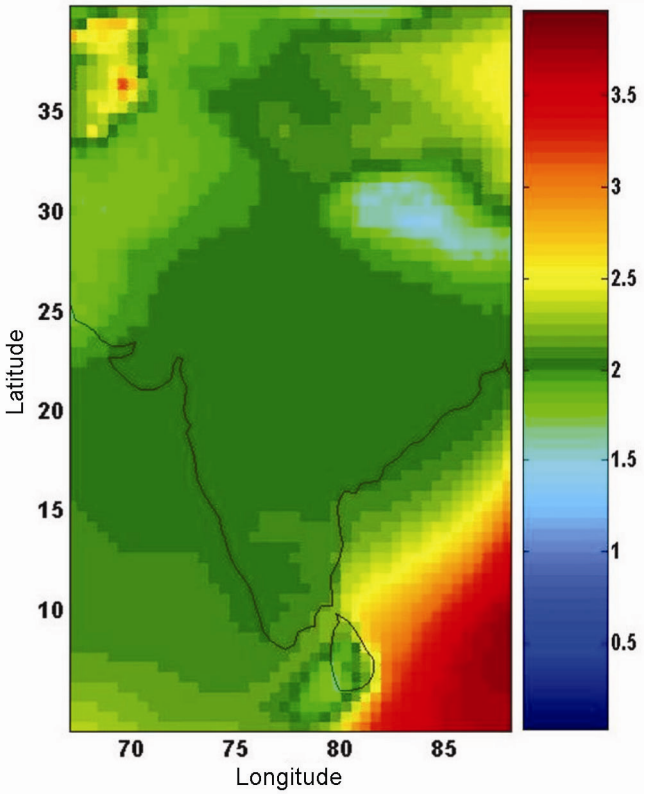

Figure 4. Fine features of spatial heterogeneity in OC/BC over Indian continent and adjacent oceanic region for January (2006–2008).

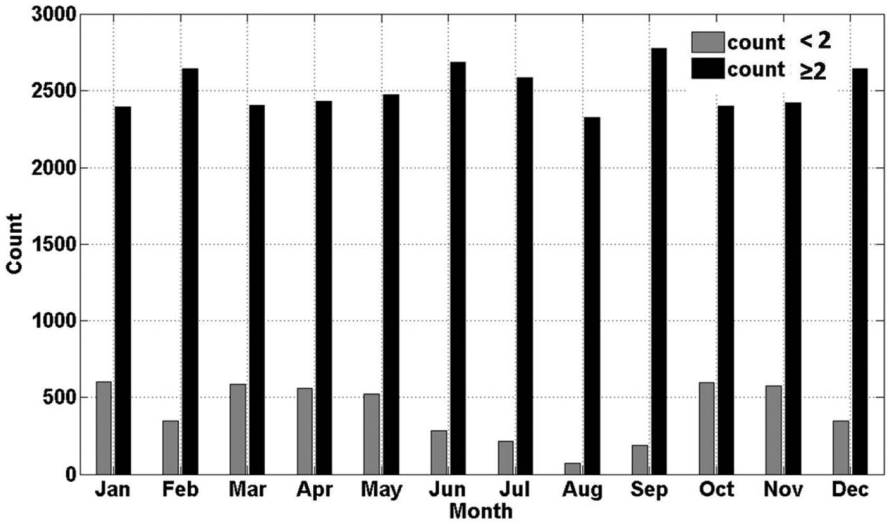

Figure 5. Pictorial representation for the count of OC/BC less than and greater than over Indian continent and adjacent oceanic region 2006–2008.

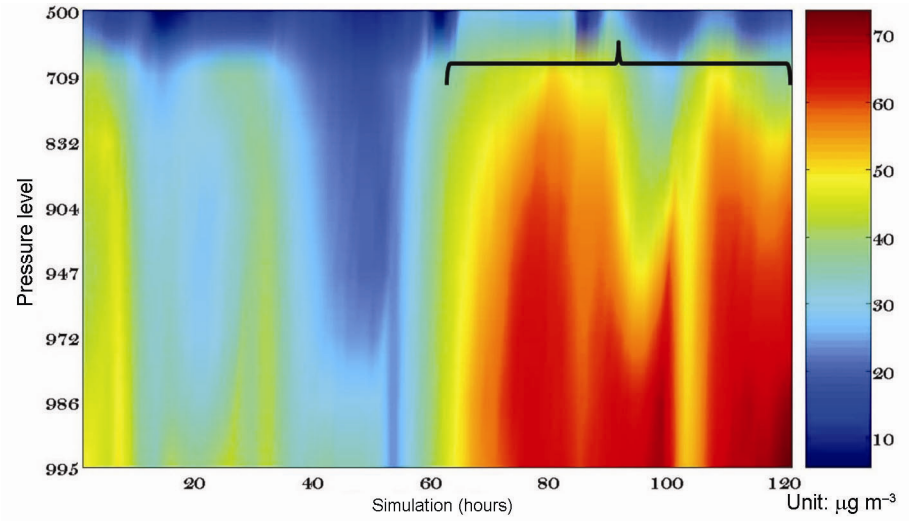

Figure 6. Simulation of dust event over a typical location in Indo-Gangetic basin, Kanpur, during 15 May 2008, i.e. after 65 h (simulation shown here for 120 h, i.e. from 12 May 2008 to 16 May 2008).

Dust storm episodes. With a view to evaluating the model's capability to capture specific episodes, we took up the case of a reported dust storm over Kanpur on 15 May 2008. Model simulations were carried out of the vertical distribution of dust concentration over Kanpur for the period from 12 May 2008 to 16 May 2008 and the results are shown in Figure 6. A clear enhancement in the concentration through higher levels is seen after around 72 h of the start (i.e. 15 May 2008) (from ~30 μg m^{-3} to more than 70 μg m^{-3}) at ground level and ~50 μg m^{-3} at higher levels (~700 hPa). This high concentration of dust persisted for next day also. This indicates the capability of CHIMERE to capture specific space and time events over Indian domain. Having simulated the spatio-temporal variation of PM_{10} and BC, with the spatial patterns in general concurrence with earlier reported patterns, we now evaluate the simulations more quantitatively by comparing them with measurements in part-II of this article.

Conclusions

We have simulated the aerosol field over the Indian (South Asian) domain (4–37.5°N; 67–88.5°E) using the chemical transport model 'CHIMERE' over a three-year period and the spatial and temporal heterogeneity of PM_{10}, BC mass concentration and the OC/BC are examined. Model simulations are made for three consecutive years, 2006, 2007 and 2008. The major findings of the study are:

- The simulated spatial distribution shows that the model is able to capture the broad features of the regional pattern of distribution of aerosols. The most dominant

feature of the spatial distribution is the high concentration of aerosols over the Indo-Gangetic basin, and this was well simulated by the model.

- This study indicates the ability of CHIMERE model to simulate aerosol loading over Indian domain.

1. Moorthy, K. K. *et al.*, Wintertime spatial characteristics of boundary layer aerosols over peninsular India. *J. Geophys. Res.*, 2005, **110**(D8), 1–11; art. no. D08207; doi: 10.1029/2004JD005520.
2. IPCC, Climate Change 2013, The Physical Science Basis, Working Group I Contribution to the Fifth Assessment Report of the Intergovernmental Panel on Climate Change, 2013.
3. Kaufman, Y. J., Tanré, D. and Boucher, O., A satellite view of aerosols in the climate system. *Nature*, 2002, **419**, 215–223.
4. Satheesh, S. K. *et al.*, Chemical, microphysical and radiative properties of Indian Ocean aerosols. *J. Geophys., Res*., 2002, **107**(23), 4725; doi: 10.1029/2002JD002463.
5. Bessagnet, B. *et al.*, Aerosol modeling with CHIMERE – preliminary evaluation at the continental scale. *Atmos. Environ*., 2004, **38**, 2803–2817.
6. Reynolds, S. D., Roth, P. M. and Seinfeld, J. H., Modeling of photochemical air pollution – I. Formulation of the model. *Atmos. Env.*, 1973, 1033–1061.
7. Hodzic, A., Modélisation Des Aérosols De Pollution En Ile-De-France, Ph D thesis, 2005.
8. Meng, Z., Dabdub, D. and Seinfeld, J. H., Size-resolved and chemically resolved model of atmospheric aerosol dynamics. *J. Geophys. Res*., 1998, **103**, 3419–3435.
9. Moorthy, K. *et al.*, Performance evaluation of chemistry transport models over India. *Atmos. Environ*., 2013, **71**, 210–225.
10. Schmidt, H., Derognat, C., Vautard, R. and Beekmann, M., A comparison of simulated and observed ozone mixing ratios for the summer of 1998 in Western Europe. *Atmos. Environ*., 2001, **35**(36), 6277–6297.
11. Vautard, R., Beekmann, M., Roux, J. and Gombert, D., Validation of a hybrid forecasting system for the ozone concentrations over the Paris area. *Atmos. Environ.*, 2001, **35**, 2449–2461.
12. Vautard, R. *et al.*, Paris emission inventory diagnostics from ESQUIF airborne measurements and a chemistry transport model. *J. Geophys. Res*., 2003, **108**(D17), doi: 10.1029/2002JD002797.
13. Hodzic, A. *et al.*, Evolution of aerosol optical thickness over Europe during the August 2003 heat wave as seen from CHIMERE model simulations and POLDER data. *Atmos. Chem. Phys*., 2006, **6**, 1853–1864.
14. Honoré, C. *et al.*, Predictability of European air quality: assessment of 3 years of operational forecasts and analyses by the PREV'AIR system. *J. Geophys. Res.*, 2008, **113**, D04301; doi: 10.1029/2007JD008761.
15. Vivanco, M. G., Palomino, I., Vautard, R., Bessagnet, B., Martín, F., Menut, L. and Jiménez, S., Multi-year assessment of photochemical air quality simulation over Spain. *Environ. Modelling Software*, 2009, **24**, 63–73.
16. Hodzic, A. *et al.*, Modeling organic aerosols during MILAGRO: importance of biogenic secondary organic aerosols. *Atmos. Chem. Phys*., 2009, **9**, 6949–6981.
17. Hodzic, A., Jimenez, J. L., Madronich, S., Canagaratna, M. R., DeCarlo, P. F., Kleinman, L. and Fast, J., Modeling organic aerosols in a megacity: potential contribution of semi-volatile and intermediate volatility primary organic compounds to secondary organic aerosol formation. *Atmos. Chem. Phys.*, 2010, **10**, 5491–5514; doi: 10.5194/acp-10-5491-2010.
18. Menut, L. *et al.*, CHIMERE 2013: a model for regional atmospheric composition modeling. *Geosci. Model Dev.*, 2013, **6**, 981–1028.
19. Ginoux, P., Chin, M., Tegen, I., Prospero, J. M., Holben, B., Dubovik, O. and Lin, S.-J., Sources and distributions of dust aerosols simulated with the GOCART model. *J. Geophys. Res.*, 2001, **6**, 20255–20273.
20. Valari, M. and Menut, L., Does an increase in air quality models resolution bring surface ozone concentrations closer to reality? *J. Atmos. Ocean. Technol*., 2008, **25**, 1955–1968; doi: 10.1175/2008JTECHA1123.1.
21. Hansen, M. C. and Reed, B., A comparison of the igbp discover and university of maryland 1 km global land cover products. *Int. J. Remote Sensing*, 2000, **21**, 1365–1373.
22. Colella, P. and Woodward, P. R., The piecewise parabolic method (PPM) for gas-dynamical simulations. *J. Comput. Phys.*, 1984, **11**, 38–39.
23. Van Leer, B., Towards the ultimate conservative difference scheme, V A second order sequel to Godunov's method. *J. Comput. Phys*., 1979, **32**, 101–136.
24. Troen, I. and Mahrt, L., A simple model of the atmospheric boundary layer: sensitivity to surface evaporation. *Bound.-Layer Meteorol*., 1986, **37**, 129–148.
25. Gelbard, F. and Seinfeld, J. H., Simulation of multicomponent aerosol dynamics. *J. Colloid Interf. Sci.*, 1980, **78**, 485–501.
26. Wesely, M., Parameterization of surface resistances to gaseous dry deposition in regional scale numerical models. *Atmos. Environ.*, 1989, **23**, 1293–1304.
27. Seinfeld, J. H. and Pandis, S. N., *Atmospheric Chemistry and Physics: From Air Pollution to Climate Change*, Wiley-Interscience, 1997.
28. Seinfeld, J. H. and Pandis, S. N., *Atmospheric Chemistry and Physics: From Air Pollution to Climate Change*, Wiley, New York, 1998.
29. Di Girolamo, L. *et al.*, Analysis of multi-angle imaging spectroradiometer (MISR) aerosol optical depths over greater India during winter 2001–2004. *Geophys. Res. Lett.*, 2004, **31**, L23115; doi: 10.1029/2004GL021273.
30. Prasad, A. K., Singh, R. P. and Singh, A. X., Variability of aerosol optical depth over Indian Subcontinent: trend and departures in recent years. *J. Indian Soc. Remote Sensing*, 2004, **32**(4), 313–316.
31. Prasad, A. K., Singh, R. P. and Kafatos, M., Influence of coal based thermal power plants on aerosol optical thickness in the Indo-Gangetic basin. *Geophys. Res. Lett.*, 2006, **33**, L05805; doi: 10.1029/2005GL023801.
32. Ramanathan, V. and Ramana, M. V., Persistent, wide spread, and strongly absorbing haze over the Himalayan foothills and the Indo-Gangetic basin. *Pure Appl. Geophys.*, 2005, **162**, 1609–1626; doi: 10.1007/s00024-005-2685-8.
33. Nair, V. S., Moorthy, K. K. and Alappattu, D. P., Wintertime aerosol characteristics over the Indo-Gangetic Plain (IGP): impacts of local boundary layer processes and long-range transport. *J. Geophys. Res.*, 2007, **112**, D13205.
34. Henriksson, S. V., Laaksonen, A., Kerminen, V.-M., Räisänen, P., Järvinen, H., Sundström, A.-M. and de Leeuw, G., Spatial distributions and seasonal cycles of aerosols in India and China seen in global climate-aerosol model. *Atmos. Chem. Phys. Discuss*., 2011, **11**, 4017–4057; doi: 10.5194/acpd-11-4017-2011.
35. Tindale, N. and Pease, P., Aerosols over the Arabian Sea, doi: 10.1594/PANGAEA.736653; Supplement to: Tindale, N. and Pease, P., Aerosols over the Arabian Sea: Atmospheric transport pathways and concentrations of dust and sea salt. Deep Sea Research, Part II: Topical Studies in Oceanography, 1999, **46**(8–9), 1577–1596; doi: 10.1016/S0967-0645(99)00036-3.
36. Li, F. and Ramanathan, V., Winter to summer monsoon variation of aerosol optical depth over the tropical Indian Ocean. *J. Geophys. Res.*, 2002, **107**(D16), 4284; 10.1029/2001JD000949.
37. Satheesh, S. K., Srinivasan, J., Vinoj, V. and Chandra, S., New directions: how representative are aerosol radiative impact assessments? *Atmos. Environ.*, 2006, **40**, 3008–3010.

38. Schwartz, J., Air pollution and hospital admissions for respiratory disease. *Epidemiology*, 1996, **7**(1), 20–28.
39. Pope III, C. A., Burnett, R. T., Thun, M. J., Calle, E. E., Krewski, D., Ito, K. and Thurston, G. D., Lung cancer, cardiopulmonary mortality and long-term exposure to fine particulate air pollution. *J. Am. Med. Assoc.*, 2002, **287**, 1132–1141.
40. Schwartz, J. *et al.*, Traffic related pollution and heart rate variability in a panel of elderly subjects. *Thorax*, 2005, **60**(6), 455–461.
41. WHO, *Fuel for Life: Household Energy and Health*, World Health Organization, Geneva, 2006, p. 43.
42. Schwartz, J. *et al.*, The effect of dose and timing of dose on the association between airborne particles and survival. *Environ. Health Perspect.*, 2008, **116**, 64–69.
43. Ganguly, D. *et al.*, Wintertime aerosol properties during foggy and nonfoggy days over urban center Delhi and their implications for shortwave radiative forcing. *J. Geophys. Res.*, 2006, **111**, D15217.
44. Pant, P. *et al.*, Study of aerosol black carbon radiative forcing at a high altitude location. *J. Geophys. Res.*, 2006, **111**(D17), D17206; doi: 10.1029/2005JD006768.
45. Ramachandran, S. *et al*., Aerosol radiative forcing during clear, hazy, and foggy conditions over a continental polluted location in north India. *J. Geophys. Res.*, 2006, **111**, D20214.
46. Srivastava, M. K. *et al.*, Direct solar ultraviolet irradiance over Nainital, India, in the central Himalayas for clear-sky day conditions during December 2004. *J. Geophys. Res.*, 2006, **111**, D08201.
47. Niranjan, K., Sreekanth, V., Madhavan, B. L. and Moorthy, K. K., Winter time aerosol characteristics at a north Indian site Kharagpur in the Indo-Gangetic plains located at the outflow region into Bay of Bengal. *J. Geophys. Res.*, 2006, **111**, D24209; doi: 10.1029/2006JD007635.
48. Niranjan, K. *et al.*, Aerosol physical properties and radiative forcing at the outflow region from the Indo-Gangetic plains during typical clear and hazy periods of wintertime. *Geophys. Res. Lett.*, 2007, **34**, L19805.
49. Rengarajan, R., Sarin, M. M. and Sudheer, A. K., Carbonaceous and inorganic species in atmospheric aerosols during wintertime over urban and high-altitude sites in North India. *J. Geophys. Res.*, 2007, **112**, D21307; doi: 10.1029/2006JD008150.
50. Beegum, S. N. *et al.*, Spatial distribution of aerosol black carbon over India during pre-monsoon season. *Atmos. Environ*., 2009, **43**, 1071–1078.
51. Bice, *et al.*, *Black Carbon, A Review and Policy Recommendations*, Princeton University, Woodrow Wilson School of Public and International Affairs; January 2009; http://www.wws.princeton.edu/research/PWReports/F08/wws591e.pdf
52. Black Carbon Research Initiative, National Carbonaceous Aerosols Programme (NCAP) Science Plan INCCA: Indian Network for Climate Change Assessment, 2011.
53. Cachier, H., *Carbonaceous Combustion Aerosols*. In *Atmospheric Particles* (eds Harrison, R. M. and Van Grieken, G. R.), 1998, pp. 295–348.
54. Satheesh, S. K. *et al.*, A model for natural and anthropogenic aerosols over the tropical Indian Ocean derived from INDOEX data. *J. Geophys. Res.*, 1999, **104**(D22), 27421–27440; doi: 10.1029/1999JD900478.
55. Bond, T. C., Street, D. G., Yarber, K. F., Nelson, S. M., Woo, J.-H. and Klimont, Z., A technology-based global inventory of black and organic carbon emissions from combustion. *J. Geophys. Res.*, 2004, **109**, D14203; doi: 10.1029/2003JD003697.
56. Novakov, T., Menon, S., Kirchstetter, T. W., Koch, D. and Hansen, J. E., Aerosol organic carbon to black carbon ratios: analysis of published data and implications for climate forcing. *J. Geophys. Res.*, 2005, **110**, D21205; doi: 10.1029/2005JD005977.

doi: 10.18520/cs/v111/i1/76-82